Structural, vibrational spectra and normal coordinate analysis for two tautomers of 4(5)-(2′-furyl)-imidazole

ARTICLE *in* JOURNAL OF RAMAN SPECTROSCOPY · MAY 2009

Impact Factor: 2.67 · DOI: 10.1002/jrs.2482

5 AUTHORS, INCLUDING:

J. J. López González
Universidad de Jaén
134 PUBLICATIONS **1,138** CITATIONS
SEE PROFILE

Aída Ben Altabef
National Scientific and Technical Research …
98 PUBLICATIONS **746** CITATIONS
SEE PROFILE

Silvia A Brandán
National University of Tucuman
123 PUBLICATIONS **897** CITATIONS
SEE PROFILE

Research Article

Journal of RAMAN SPECTROSCOPY

Received: 17 April 2009 Accepted: 9 August 2009 Published online in Wiley Interscience: 19 October 2009

(www.interscience.wiley.com) DOI 10.1002/jrs.2482

Structural, vibrational spectra and normal coordinate analysis for two tautomers of 4(5)-(2′-furyl)-imidazole

A. E. Ledesma,[a] J. Zinczuk,[b†] J. J. López González,[c] A. Ben Altabef[a†] and S. A. Brandán[a*]

We have synthesized both the 4 and 5 tautomeric forms of 4(5)-(2′-furyl)-imidazole (1) and investigated their molecular vibrations by infrared and Raman spectroscopies as well as by calculation based on the density functional theory (DFT) approach. Examination of the temperature dependence of IR intensity revealed the band characteristics of the 4 and 5 tautomers of (1). Comparison of experimental and calculated chemical shifts in nuclear magnetic resonance (NMR) spectroscopy was made in order to identify the two tautomeric forms. The assignment of vibrational normal modes was performed, and the force field obtained reproduced the experimental vibrational wavenumbers with a root mean-square deviation (RMSD) value of *ca*. 13 cm^{-1} for both tautomers. The natural bond orbital (NBO) study reveals the characteristics of the electronic delocalization of the two tautomeric structures.

Supporting information may be found in the online version of this article.

Keywords: 4(5)-(2′-furyl)-imidazole; DFT calculation; infrared spectrum; Raman spectrum; tautomeric structures; force field

Introduction

Since 1970, there have been a number of studies on the tautomerism of imidazoles, and some aspects have been reviewed.[1–3] In the solid and liquid states, the N-unsubstituted imidazole compounds frequently exist in the associated form and they are subject to fast hydrogen exchange. In 4-substituted imidazoles that contain a free N–H bond, this rapid exchange is the responsible of the prototropic tautomerism exhibited by them. The ^{1}H NMR spectrum of those compounds exhibits only two C–H resonances with an integral ratio 2 : 1, which indicates that on the NMR timescale the H4 and H5 atoms are equivalent.[4] In fact, the imidazoles provide one of the best studied examples of annular tautomerism, and the values of the tautomeric ratio K_T have been calculated for a variety of 4(5)-substituted imidazoles and the results summarized.[2] The application of the Hammett equation to heteroaromatic tautomerism by Charton[5,6] has suggested qualitatively that the electron-donating groups ($\sigma_m < 0$) will favor the 5-sustituted isomer whereas the electron-withdrawing groups ($\sigma_m > 0$) will favor the 4-substituted tautomer. Recently it was found that new 4(5)-imidazole derivatives, their stereoisomers, and their non-toxic pharmaceutically acceptable acid addition salts exhibit selective aromatase-inhibiting properties.[7] Many studies in recent years have dealt with the synthesis and tautomeric equilibrium related to aryl imidazoles.[8–10] Thus, Talbot *et al*.[11] using the loan laser system (LSF) have studied the electronic spectra of jet-cooled 4-phenylimidazole, its singly hydrated complex, as well as its tautomer, 5-phenyl imidazole. Furthermore, the phenyl ring of 4-phenylimidazole provides a suitable chromophore to examine hydrogen bonding to the imidazole group, and 4-phenylimidazole is itself an enzyme inhibitor.[12] Vázquez *et al*.[13] have presented a theoretical structural and vibrational study on (2′-furyl)-imidazole series, in which the two conformers of the 4-(2′-furyl)-imidazole and 5-(2′-furyl)-imidazole molecules were analyzed using *ab initio* Hartree–Fock (HF) and second-order perturbation Möller–Plesset (MP2) calculations. In the present work, we report an experimental and theoretical vibrational study of 4(5)-(2′-furyl)-imidazole by means B3LYP calculations using 6-31G* and 6-311++G** basis sets. For a complete assignment of the compound, the DFT calculations were combined with the scaled quantum mechanical force field (SQMFF) methodology[14–16] in order to fit the theoretical wavenumbers to the experimental ones. The changes in the chemical shifts of the hydrogen and carbon atoms in the tautomeric equilibrium were also studied. In addition, the electronic properties of both tautomers of the compound were evaluated by natural bond orbital(NBO)[17–20] and atoms in molecules (AIM)[21,22] studies in order to analyze the nature and magnitude of the intramolecular interactions.

* *Correspondence to: S. A. Brandán, Instituto de Química Física, Facultad de Bioquímica, Química Y Farmacia, Universidad Nacional de Tucumán, San Lorenzo 456, T 4000 CAN, San Miguel de Tucumán. Tucumán, R. Argentina. E-mail: sbrandan@fbqf.unt.edu.ar*

† *Member of the Carrera de Investigador Científico, CONICET, R. Argentina.*

a *INQUINOA-CONICET, Instituto de Química Física, FBQyF, Universidad Nacional de Tucumán, San Lorenzo 456, T 4000 CAN, Tucumán, R. Argentina*

b *Instituto de Química Rosario (CONICET-UNR), Facultad de Ciencias Bioquímicas y Farmacéuticas, Suipacha 531, Santa Fé, R. Argentina*

c *Departamento de Química Física y Analítica, Facultad de Ciencias Experimentales, Universidad de Jaén, 23071 Jaén, Spain*

Experimental

Synthesis

4(5)-(2′-furyl)-imidazole (**1**) was synthesized using the following precursors:

Sulfonamide

In a 250-ml flask with three mouths, 90 ml aqueous ammonium hydroxide was placed (1.2 mol).[23] While stirring with magnetic stirrer, 30 g of finely divided *p*-toluenesulfonyl chloride (0.157 mol) was added. The mixture was heated under reflux for 1 h. The resulting product was filtered, recrystallized from water, and dried in an oven. w: 25.5 g; m.p: 137–138 °C; yield: 95%.

N-Tosylbenzaldimine

Under a nitrogen atmosphere, 25.5 g (0.15 mol) of sulfonamide and 4 g (12.4 ml) (0.15 mol) of furfuraldehide purified by fractional distillation were made to react in presence of $Si(EtO)_4$ 32.7 g (0.157 mol).[24] The mixture was allowed to boil in a silicone oil bath at 164 °C for 1h. The dark product was dissolved in 125 ml of hot ethyl acetate with agitation and the resulting solution was made colorless with activated charcoal. The filtrate was diluted with 600 ml of hexane. The insoluble solid was separated, filtered, and dried to give a yellowish crystalline solid. w: 18.97 g. yield: 50.7%. m.p: 97.3–99.3 °C. Finally, the product was purified by crystallization in AcOEt–hexane. m.p: 101.3–102.7 °C.

4(5)-(2-furyl)-imidazole

A mixture of TosMIC (98%) 6.58 g (33 mmol), *N*-tosyl benzaldimine 7.50 g (30 mmol), K_2CO_3 9.10 g (66 mmol), and MeOH/DME 2 : 1 (300 ml) was heated under reflux with stirring for 1 h.[25] It was cooled down to room temperature (RT), and 100 of cold water was added and then all the mixture stirred for 15 min. The reddish solution was diluted with 500 ml of cold water; it was extracted successively with 400 ml of ethyl ether and with 500 ml of CH_2Cl_2. The organic phases were collected and concentrated under reduced pressure. The residue (6.17 g) was dissolved in HCl 3 N (500 ml), alkalinized with aqueous 50% NaOH (pH=8), and extracted with CH_2Cl_2 (2 × 150 ml). The collected organic phase was washed with NaCl saturated solution, dried with $MgSO_4$, and filtered and concentrated under reduced pressure. The resulting product (1.87 g, dark oil) was purified by column chromatography (alumina 507 C, 100–125 mesh, pH: 7) with CH_2Cl_2 as solvent using a Redifrac collector (fractions × 2000 drops). w: 0.61 g.

The product was dissolved in 50 ml of ether and stirred for 3 h at RT with addition of NaOH 12.5 N (35 ml) solution. The aqueous phase was neutralized with H_2SO_4 12 N, extracted with ether (3 × 20 ml), dried with $MgSO_4$, filtered, and evaporated. A light brown solid resulted. w: 284 mg, yield: 7%. On sublimation of the product (95 mg) at 100 °C at 0.5 Torr, 90 mg of white solid was obtained. m.p.: 112.8–113.4 °C. On crystallization in CH_2Cl_2, the m.p. rises to 115–116 °C.

The Raman spectra of the solid as well as the FTIR spectra at RT and low temperatures (LT) were registered. The infrared spectrum of the solid 4(5)-(2′-furyl)-imidazole in KBr pellets from 4000 to 200 cm^{-1} at RT was recorded on an FTIR GX1 spectrophotometer, equipped with a globar source and a DGTS detector at a resolution of 1 cm^{-1} and 64 scans. The infrared spectra between 4000 and 200 cm^{-1} at LT were registered on an FTIR Digilab model 14 spectrophotometer in KBr pellets using the RCII (VLT-2) cell. The Raman spectrum (resolution 1 cm^{-1}, 200 scans) was recorded with a Bruker RF100/S spectrometer equipped with a Nd : YAG laser source (excitation line 1064 nm, 800 mW power) and a Ge detector. Nuclear magnetic resonance (NMR) spectra were recorded for dilute solutions in $CDCl_3$ using a Bruker 400 FT spectrometer at 400 MHz for ^1H and 100 MHz for ^{13}C. The ^1H NMR spectra were also registered at 273, 263, 253, 243 K with the same spectrometer. GC-MS spectra were recorded with a Perkin Elmer Autosystem XL Gas Chromatograph Turbomass Mass Spectrometer, using a nonpolar (100% polidimethylsiloxane) column (SE-30, 25 m × 0.22 mm i.d).

Computational details

The DFT calculations for the compound were performed using the Gaussian 03 program package[26] with the 6-31G* and 6-311++G** basis sets and the hybrid B3LYP functional approach.[27,28] The force fields in Cartesian coordinates were calculated for all conformations of the compound at B3LYP/6-31G* and B3LYP/6-311++G** levels. The resulting force fields were transformed to 'natural' internal coordinates with the MOLVIB program.[29,30]

The natural coordinates are shown in Table S1 (Supporting Information), which were defined as proposed by Pulay *et al*.[31,32] Following the SQMFF procedure,[14–16] the harmonic force field was scaled using the recommended scaling factors of Rauhut and Pulay.[14,15] The calculated chemical shifts of the ^1H NMR and ^{13}C NMR for the two tautomers were obtained by means the GIAO method[33] using the B3LYP/6-311++G** level of theory. For all structures, an NBO analysis was performed using the NBO 3.1 program,[20] while the topological properties and the nature and magnitude of the intramolecular interactions were also studied by means the AIM2000 program.[22]

Result and Discussion

Geometrical optimization

For each tautomeric structure of **1**, which are 4-(2′-furyl)-imidazole (**4-FI**) and 5-(2′-furyl)-imidazole (**5-FI**), two different stables conformations were obtained according to *syn* and *anti* position of oxygen atom with respect to the C5–H9 and N1–H6 bonds, respectively, named the *syn* and *anti* conformers, respectively. The labeling of the atoms for all conformers of both tautomers is shown in Fig. 1. We can see that the *anti* conformer of the **4-FI** tautomer is in equilibrium with the *syn* conformer of the **5-FI** tautomer due to the prototautomerism, and for this reason only two structures would be expected for this compound. The theoretical calculations predict that all molecules have C_s symmetry. The calculated energy differences among both conformations of the two tautomers of **1,** with B3LYP/6-31G* and 6-311++G** levels, are shown in Table 1. For both tautomers, the *syn* conformers have lower energy and therefore are the most stable. Also, the energy difference between both conformations of each tautomer is higher for **4-FI** than for the other tautomer. The calculated parameters for **4-FI** and **5-FI** tautomers using the B3LYP level at different basis sets compared with the experimental X-ray data for the 2-(2′-furyl)-1*H*-imidazole compound[34] are listed in Table 2. There are no significant differences between the observed calculated geometric parameters for all conformers of both tautomers. The analysis of these parameters show that the calculated distances and bond angles are very close to the experimental ones, with

Journal of RAMAN SPECTROSCOPY

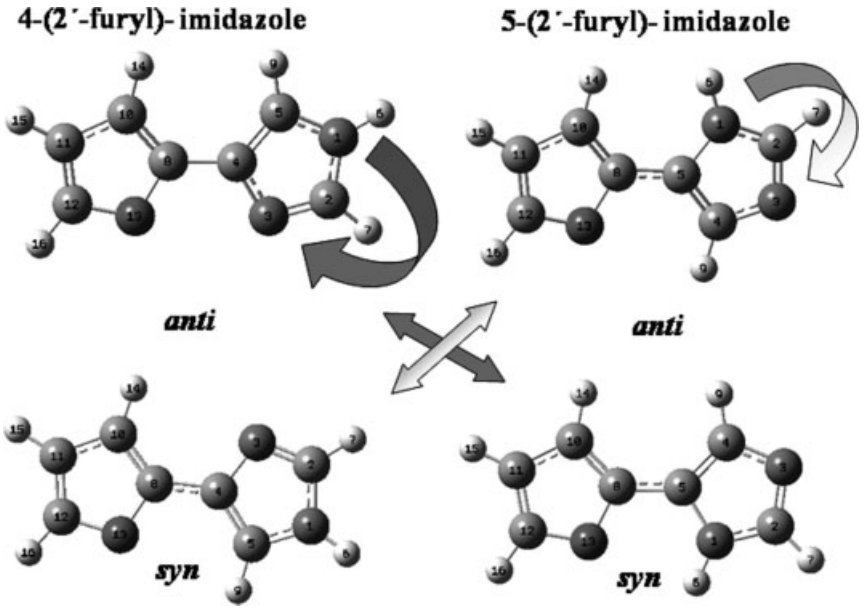

Figure 1. Theoretical structures and atoms numbering of the 4 and 5 tautomers of 4(5)-(2′-furyl)-imidazole. The proton tautomerism is indicated with arrows.

the root mean-square deviation (RMSD) values of 0.02 Å for the distances and of 1.2° for the angles. The slight differences between the calculated N3–C4 and N3–C2 distances are attributed, in the first case, to the experimental value because in the 2-(2′-furyl)-1*H*-imidazole compound[34] the resultant value is an average of single and double bonds, while the theoretical value of the N3–C2 distance corresponds to a pure coordinate. Also, the calculated N3–C4 distance (*ca*. 1.384 Å) is significantly smaller than the N–C single bond (sum of the N and C covalent radii is 1.52 Å),[35] suggesting a substantial degree of electron delocalization on the imidazole ring.[36] On the other hand, the C–C inter-ring bond length is higher for both tautomers (**4-FI** and **5-FI)** compared to the 2-(2′-furyl)-1*H*-imidazole compound, showing that both rings are more separated in those tautomers than in the latter. Moreover, the larger calculated C═C lengths for both tautomers justify the lower conjugation effects between the furane and imidazole rings. Significant changes are not observed for the bond angles.

NMR

Figure S1 (Supporting Information) shows the ^{1}H NMR spectrum of **1** in deuterated chloroform. Three signals corresponding to three different H atoms of the imidazole ring are observed. The corresponding calculated and experimental chemical shifts for the H and C atoms appear in Table 3. The peaks at 6.43, 6.54, and 7.39 ppm belong to three H atoms on 14, 15, and 16 positions of the furane rings, respectively, while the peaks at 7.33 and 7.71 ppm belong to two H atoms on position 9 and 7 of the imidazole rings, respectively. These chemical shift values are in agreement with those in the literature.[37,38] The peak belonging to H atom of the N–H bond appears at 11.37 ppm. A small shift of these peaks towards lower fields implies the existence of some intermolecular interaction between nonbonding electrons. As seen in Fig. S1 (Supporting Information), the broad peak associated with the H atom of the N–H group of the imidazole ring appears at 11.37 ppm because the H atom is exchanged between two imidazole rings via the intermolecular hydrogen bond, and so the H atom of the N–H bond peak is slightly shifted to lower fields with respect to that of the imidazole molecule. These chemical shift values indicate that in 4(5)-(2′-furyl)-imidazole the H atom is held weakly by two imidazole rings. At an intermediate rate of exchange, the H atom is partially decoupled, and a broad N–H peak results. Figure S2 (Supporting Information) shows the ^{13}C NMR spectrum of **1** in deuterated chloroform. The most intense peak of this spectrum belongs to the C atom of the reference, while the following four peaks belong to the C atoms of the furyl group. The peak at 135.62 ppm belongs to the C2 atom of the imidazole ring and the two peaks of smaller intensity belong to the C5 and C4 atoms of this ring. The calculated chemical shifts are in agreement with the experimental ones, with RMSD values of 2.53 and 0.32 ppm for the ^{13}C and ^{1}H atoms, respectively. The agreement with our experimental data in these solvents is good, except for the H atom of the H–N bond in chloroform. This is because the calculations are for the gas phase, while the experimental values are for the $CDCl_3$ solution where the molecular interactions are important. It is important to mention that the registered NMR spectra at RT and LT were not sufficient to identify the tautomeric mixture of **1**, because the speed of exchange of protons is higher than the response time of NMR.

NBO and AIM analyses

The stability of the two tautomers of **1** was investigated by NBO calculations.[17–19] The second-order perturbation energies $E^{(2)}$ (donor → acceptor) that involve the most important delocalization stabilization energies ($E^{(2)}$, in kJ/mol) associated with the main delocalizations for all structures of 4(5)-(2′-furyl)-imidazole are given in Table 4. We found that the contributions of the stabilization energies for the σN1-C5→ σ^*C4–C8 charge transfers are higher for the **4-FI** tautomer than the other tautomer, while the opposite situation is observed in the stabilization energies of the σN3-C4→ σ^*C4–C8 charge transfers for the **5-FI** tautomer. Moreover, as was observed for the methylated species of 4-(2′-furyl)-imidazole,[39] the π^*C4 = C5→ π^*C8 = C10 and π^*C11 = C12→ π^*C8 = C10 charge transfers are only observed in the **4-FI** tautomer. The parameters obtained for the atoms

Table 1. Calculated total (ET) and relatives (ΔE) energies and dipole moment (μ) for 4-(2′-furyl)-imidazole (**4-FI**) and 5-(2′-furyl)-1*H*-imidazole (**5-FI**)

	DFT/B3LYP/6-31G*			
Tautomer	**4-FI**		**5-FI**	
Conformer	*anti*	*syn*	*anti*	*syn*
μ (Debye)	3.94	3.23	3.98	3.37
ET (Hartrees)	−455.0491050	−455.0537620	−455.0513554	−455.0534867
ΔE (kJ/mol)	12.20	0.0	5.60	0.0
	DFT/B3LYP/6-311++G**			
Tautomer	**4-FI**		**5-FI**	
μ (Debye)	4.12	3.24	4.17	3.42
ET (Hartrees)	−455.1753400	−455.1803045	−455.1772201	−455.1795573
ΔE (kJ/mol)	13.00	0.0	6.10	0.0

Table 2. Comparison between the calculated geometrical parameters of 4-(2′-furyl)-imidazole (**4-FI**) and 5-(2′-furyl)-imidazole with the experimental one of 2-(2′-furyl)-1*H*-imidazole (**5-FI**)

			4-FI				**5-FI**			
			6-31G*		6-311++G**		6-31G*		6-311++G**	
Parameter	Exp.[#]		*anti*	*syn*	*anti*	*syn*	*anti*	*syn*	*anti*	*syn*
Bond length (Å)										
O13–C12	1.361	(3)	1.362	1.363	1.361	1.365	1.365	1.368	1.365	1.364
O13–C8	1.363	(2)	1.367	1.366	1.364	1.370	1.369	1.374	1.367	1.367
N3–C4	1.342	(3)	1.384	1.385	1.382	1.383	1.373	1.372	1.373	1.372
N1–C5	1.374	(3)	1.378	1.379	1.377	1.378	1.385	1.384	1.385	1.385
N3–C2	1.339	(2)	1.312	1.295	1.310	1.310	1.315	1.317	1.312	1.313
N1–C2	1.369	(3)	1.367	1.367	1.366	1.366	1.366	1.365	1.367	1.366
C4–C8	1.438	(3)	1.451	1.446	1.450	1.445	1.441	1.441	1.439	1.439
C4–C5	1.345	(3)	1.381	1.379	1.379	1.377	1.382	1.383	1.380	1.380
C8–C10	1.343	(3)	1.372	1.368	1.369	1.365	1.372	1.370	1.369	1.369
C10–C11	1.413	(3)	1.430	1.431	1.429	1.432	1.431	1.431	1.431	1.431
C11–C12	1.319	(4)	1.362	1.361	1.359	1.358	1.360	1.360	1.358	1.357
RMSD (Å)			0.025	0.027	0.024	0.023	0.023	0.023	0.023	0.022
Bond angles (°)										
C12–O13–C8	106.6	(2)	107.3	106.7	107.4	107.1	107.2	107.1	107.4	107.5
C2–N1–C5	105.6	(2)	107.2	107.3	107.3	107.4	107.3	107.4	107.3	107.4
C4–N3–C2	105.7	(2)	105.5	105.4	105.8	105.7	105.3	105.3	105.7	105.7
N1–C2–N3	111.6	(2)	111.9	111.9	111.7	111.6	111.8	111.8	111.6	111.5
N3(N1)–C4–C8	123.7	(2)	122.3	121.2	122.5	121.3	123.3	122.1	123.0	123.2
N3–C4–C5	108.7	(2)	110.1	110.3	109.9	110.1	111.0	110.9	110.7	110.7
N1–C5–C4	108.4	(2)	105.3	105.1	105.3	105.1	104.4	104.3	104.6	104.5
C10–C8–O13	109.2	(2)	109.5	109.8	109.5	109.8	109.5	109.6	109.5	109.4
C10–C8–C4(5)	134.2	(2)	133.1	132.9	132.9	132.9	134.2	134.2	134.0	134.1
O13–C8–C4(5)	116.6	(2)	117.4	117.3	117.5	117.3	116.3	116.2	116.5	116.4
C8–C10–C11	107.1	(2)	106.6	106.4	106.6	106.4	106.5	106.5	106.4	106.5
C12–C11–C10	106.6	(2)	106.0)	106.3	106.1	106.4	106.2	106.5	106.3	106.3
C11–C12–O13	110.6	(2)	110.5	110.4	110.4	110.3	110.5	110.2	110.3	110.2
RMSD (°)			1.09	1.18	1.09	1.16	1.37	1.38	1.27	1.29
Dihedral angles (°)										
C10-C8-C4(C5)-N3(N1)	8.0	(4)	180	0	180	0	180	0	180	0
O13-C8- C4(C5)-N3(N1)	172.00	(17)	0	180	0	180	0	180	0	180

[#] Ref. [34].

Table 3. Calculated[a] and experimental chemical shifts (in ppm) for 4-(2′-furyl)-imidazole (**4-FI**) and 5-(2′-furyl)-imidazole (**5-FI**)

	δC		δH, multiplicity	δH
Position	Experimental[b]	Calculated[c]	Experimental[b]	Calculated[c]
10	104.31	103.55	6.54 (d, $J = 3.3$ Hz, 1H)	6.29
11	111.32	108.82	6.43 (dd, $J = 1.8$, $J = 3.3$ Hz, 1H)	6.17
5	114.68	111.03	7.33 (d, $J = 0.9$ Hz, 1H)	6.98
4	131.61	132.40		
2	135.62	138.1	7.71 (d, $J = 0.9$ Hz, 1H)	7.26
12	141.23	141.35	7.39 (dd, $J = 0.9$, $J = 1.5$ Hz, 1H)	7.16
8	148.99	153.20		
N-H	–	–	11.37 (bs,1H)	7.86

[a] B3LYP/6-311++G**, average value of the two tautomers.
[b] In Cl_3DC.
[c] Ref to TMS.

Table 4. Stabilization energies ($E^{(2)}$, in kJ/mol) associated with main delocalization for all studied structures of 4(5)-(2′-furyl)-imidazole

B3LYP/6-311++G**				
	4-FI		**5-FI**	
$E^{(2)}$ (donor → acceptor)	*anti*	*syn*	*anti*	*syn*
σN1–C5→ σ* C4–C8	16.47	17.14	4.93	7.98
σC2–N3→ σ* N3–C4	2.72	2.84	2.30	–
σN3–C4→ σ* C4–C8	6.02	6.69	16.85	15.42
σC4–C5→ σ* C4–C8	14.30	14.42	19.65	14.42
πC2–N3→ π* C4–C5	89.70	87.78	84.77	79.88
πC4–C5→ π* C2–N3	62.57	62.95	65.75	84.02
πC4–C5→ π* C8–C10	56.64	62.37	67.84	72.94
πC8–C10→ π* C4–C5	58.19	66.38	57.18	52.25
πC8–C10→ π* C11–C12	70.18	71.44	–	70.31
π* C2–N3→ π* C4–C5	425.02	327.96	367.17	435.60
π* C4–C5→ π* C8–C10	689.32	538.01	–	–
π* C11–C12→ π* C8–C10	–	481.70	–	–

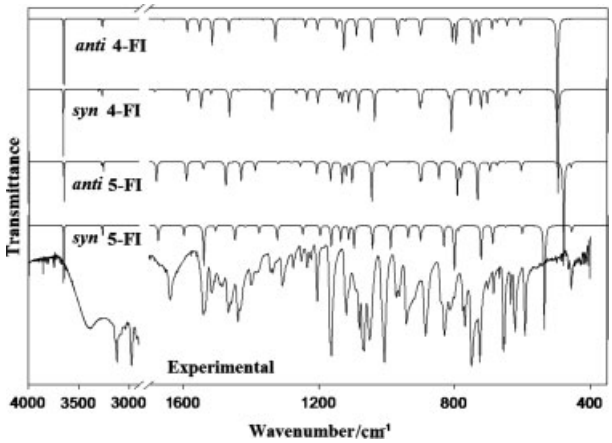

Figure 2. Infrared spectra of 4(5)-(2′-furyl)-imidazole. Upper: theoretical at B3LYP/6-311++G** level. Lower: Experimental spectrum of the solid substance.

involved in those transitions, such as the natural charges and the bond order expressed as the Wiberg bond index, are given in Table S2 (Supporting Information), whereas the polarization coefficients and percentages and population of the main orbitals for all studied structures are presented in Table S3 (Supporting Information). The results correlate well with the calculated short C8–C10 distance. A possible explanation of this observation could be the observed larger population in the bonding C4–C5 orbital of the **4-FI** tautomer in relation to other tautomer, or the larger C4–C5 bond order value in this tautomer. Also, the intramolecular interactions have been analyzed by using Bader's topological analysis of the charge electron density $\rho(r)$. The localization of the bond critical points (BCPs) in the $\rho(r)$ and the values of the Laplacian at these points are important for the characterization of the molecular electronic structure in terms of the nature of interaction and its magnitude. This BCP has the typical properties of the closed-shell interaction. When the value of $\rho(r)$ is relatively low, $|\lambda 1|/\lambda 3$ is <1 and the Laplacian of the electron density $\nabla^2\rho(r)$ is positive, which indicates that the interaction is dominated by the contraction of charge away from the interatomic surface toward each nucleus.[40–47] In this study, only the 6-311++G** basis set has been considered because there are numerous references where the quality of the basis set was found to have no influence on the topological results.[48,49] It is important to note that there is no BCP in all conformers of **1** with typical properties of the closed-shell interaction. The analysis of the ring critical point (RCP) is reported in Table S4 (Supporting Information), and the electronic densities in the BCPs as well as the large negative values of $\nabla^2\rho(r)$ for the C4–C5, C8–C10, C11–C12 distances in all conformers of **1** are in agreement with the obtained values for covalent bonding, as expected (Table S5, Supporting Information). In this study, two correlations in the topological properties of those BCPs are observed. The first correlation is between the negative values of $\nabla^2\rho(r)$ and the charge electron density $\rho(r)$ corresponding to those C–C distances (Table S6, Supporting Information), while the second one is between the $\nabla^2\rho(r)$ and $\rho(r)$ corresponding to RCP of all conformers of **1** (Table S7, Supporting Information). The relations are completely linear in both cases. It means that the properties of the C–C BCPs may be very useful to estimate the strength of the intramolecular C–C bond.

Vibrational results

The experimental infrared and Raman spectra at RT of **1** are shown in Figs 2 and 3, respectively, revealing a rather complex composition of the vibrational bands for this compound. The two

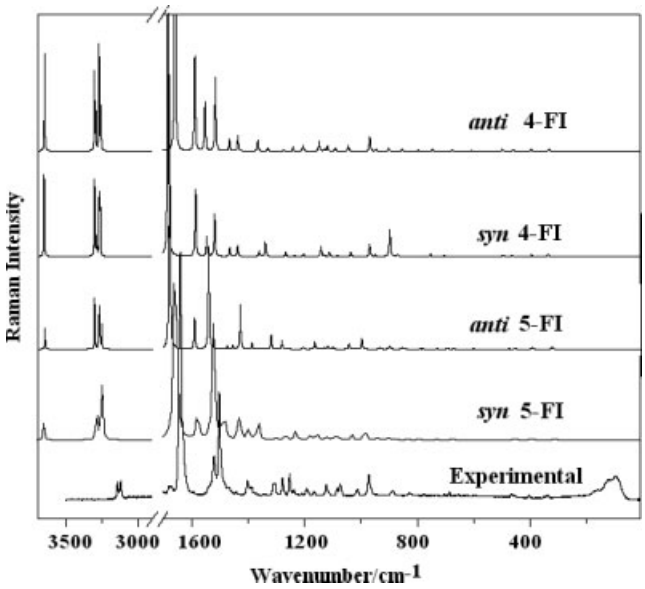

Figure 3. Raman spectra of 4(5)-(2′-furyl)-imidazole. Upper: theoretical at B3LYP/6-311++G** level. Lower: Experimental spectrum of the solid substance.

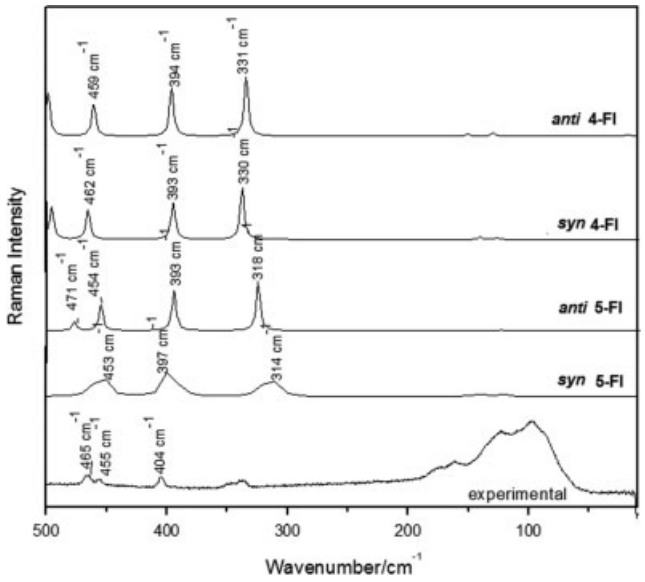

Figure 5. Raman spectra of 4(5)-(2′-furyl)-imidazole in the 500–10 cm^{-1} region. Upper: Theoretical at B3LYP/6-311++G** level. Lower: Experimental spectrum of the solid substance.

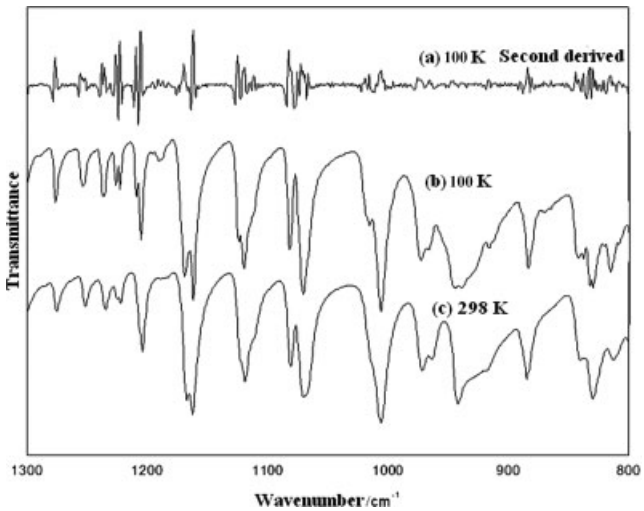

Figure 4. Infrared spectra of 4(5)-(2′-furyl)-imidazole. Infrared spectrum (a) and second derivative (b) recorded at 100 K and (c) 298 K.

conformers of both tautomers of **1** exhibit C_s symmetry and have 42 vibration modes classified as 29A′ and 13A″ vibrations and all are infrared and Raman active. The assignment of the vibrational normal modes for the two conformers of the both tautomers is shown in Table 5. An exhaustive comparison with the infrared spectrum of the methylated species of the **4-FI** tautomer[39] as well as also with the experimental assignments of similar molecules[50,51] was very useful for the assignment of the bands in this compound. Thus, the observed IR bands at 1438, 1235, 917, 769, and 635 cm^{-1} are absent in the spectrum of the methyled species of **4-FI**, and for this reason they were assigned to the **5-FI** tautomer. The experimental vibrational spectrum fits fairly well with that predicted by the theoretical model for the two tautomers. These results probably indicate the existence of a mixture of both tautomers in the solid phase. Especially, in the case of both conformers of the **4-FI** tautomer, its theoretical vibrational spectra exhibit close similarity, as shown in Figs 2 and 3. Furthermore, the analysis of the infrared spectrum at LT (100 K) allowed carrying out an assignment with a good approach showing, e.g., that the bands located at 1638, 1438, 1430, 1342, and 830 cm^{-1} in the IR spectrum at RT and LT are split. Figure 4 shows the experimental spectrum at RT in the 1300–800 cm^{-1} region compared with the corresponding spectrum at 100 K and with the second derivative curve of the spectrum at 100 K. It is important to observe that the second derivative curve clearly indicates the peak positions of IR bands in this region, as was observed by Toyama *et al.*[52] in the tautomers of 4-methylimidazole. A reasonable explanation for the observed changes at LT would be the presence in the solid of the different conformers belonging to both tautomers. According to the theoretical calculations, for the **5-FI** tautomer it is possible to observe bands assignable to each one of its two conformers separately, whereas for the **4-FI** tautomer only one band is generally observed for both conformers. For example, in the region between 800 and 700 cm^{-1} (Fig. S3, Supporting Information), the experimental spectra at 298 and 100 K show only one band at 750 cm^{-1} (298 K) and 753 cm^{-1} (100 K), which would be assignable, in accordance with the calculations, to the normal ν_{33} mode of the two conformers of **4-FI** at 752 cm^{-1}. On the other hand, the bands observed at RT at 776 and 769 cm^{-1} and at LT at 777 and 771 cm^{-1}, as well as by the calculations at 788 cm^{-1} (*syn*) and 776 cm^{-1} (*anti*), can also be assigned to ν_{33} for both conformers of **5-FI**, although for the ν_{32} mode of the conformer *anti* of this tautomer the value calculated at 789 cm^{-1} is overlapped with the band corresponding to the ν_{33} of the *syn* conformer. Also, a similar argument can be made for the ν_8 mode in the 1550 and 1500 cm^{-1} region (Fig. S3, Supporting Information). For this mode, in the *syn* and *anti* conformers of **4-FI** a single band is observed at 1516 cm^{-1} in the spectrum at RT and at 1521 cm^{-1} in the spectrum at 100 K, which can be compared with the calculated values for those conformers of **4-FI** at 1507 cm^{-1}. On the other hand, the two peaks of this band appear better resolved at RT at 1538 and 1534 cm^{-1} (298 K) and at 1542 and 1530 cm^{-1} (100 K),

Table 5. Assignments of bands of 4(5)-(2′-furyl)-imidazole

				4-FI				5–FI				
				anti		*syn*		anti		syn		
	IR R. T.[a]	IR L.T.[b]	Raman	Calc.[c]	SQM[d]	Calc.[c]	SQM[d]	Calc.[c]	SQM[d]	Calc[c].	SQM[d]	Assignment[e]
Symmetry A′												
ν_1	3442 br	–		3630	3444(88.7)	3656	3443(88.9)	3656	3444(8.5)	3650	3445(64.8)	ν (N1–H6) (99)
ν_2	3141 sh	3139 w	3145 (7)	3257	3145(0.1)	3280	3145 (0.9)	3284	3145(0.2)	3284	3145(0.3)	ν (C12–H16) (86)
ν_3	–	–	–	3248	3144(1.5)	3280	3144 (0.7)	3256	3144(3.3)	3257	3144(0.1)	ν (C5–H9) (97)
ν_4	3129 w	3127 w	3123 (8)	3224	3129(0.4)	3264	3129 (0.4)	3251	3129(0.3)	3248	3129(1.8)	ν (C10–H14) (90)
ν_5	–	3119 w	–	3224	3110(1.6)	3244	3120 (1.5)	3245	3110(1.6)	3244	3110(4.2)	ν (C2–H7) (98)
ν_6	3081 w	3064 w	–	3212	3108(5.0)	3243	3108 (5.2)	3238	3108(8.0)	3243	3108(5.6)	ν (C11–H15) (84)
ν_7	1638 m	1645 w 1640 m	1639 (100)	1632	1606(2.3)	1665	1606 (2.2)	1661	1603(21.2)	1656	1596(16.9)	ν (C8═C10) (31), ν (C4–C8) (27)
ν_8	1538vs 1534 s	1542 s 1530 m	1540 (20)					1568	1514(13.4)	1576	1521(8.5)	ν (C11═C12) (26), ν (C4–N3) (16)
	1516 m	1524 sh 1521 m	1520 (18)	1561	1507(9.1)	1562	1507 (9.1)					ν (C11═C12) (42), ν (C4–N3) (14)
ν_9	1491 m	1492 m	1492 (43)	1527	1474(23.4)	1528	1471(23.5)	1521	1472(8.1)	1520	1470(37.8)	ν (N3–C2) (47), β(C2–H7) (22)
ν_{10}	1467 m 1458 w	1471 m 1455 w	1468 (3)	1488	1446(91.5)	1496	1445(6.1)					ν (C8═C10) (18), ν (C11═C12) (17), β(C5–H9) (12)
	1438 s	1443 m 1441 s	1442 (7)							1484	1438(6.6)	ν (N1–C2) (24), β (C2–H7) (22)
	1430 s	1434 m 1431 s	–					1454	1407(30.8)			β (C2–H7) (15), ν (C2–N1) (15), ν (C4-N3) (13)
ν_{11}	1400 m	1402 m 1399 w	1401 (2)	1446	1392(29.0)	1442	1386(29.0)	1437	1395(0.8)	1429	1379(11.3)	ν (C2–N1) (22), β (C12–H16) (20)
ν_{12}	1378 sh	1378 w	1371 (1)	1413	1370(0.7)	1413	1368(0.7)	1411	1369(15.0)	1397	1354(1.4)	ν (C10–C11) (22), β (C11–H15) (16)
ν_{13}	1342 m 1335 w	1342 w 1335 m	1343 (2)					1372	1327(4.6)	1362	1315(3.6)	ν (C10–C11) (15), ν (C2–N1) (15)ν (N1–C5) (22), ν (C2–N3) (15)
	1307 s 1304 m	1310 s 1304 m	1308 (6)	1344	1298(2.7)	1344	1298(2.7)					ν (N1–C5) (28), ν (C4–C5) (17), β (C2–H7) (13), ν (C2–N3) (10)
ν_{14}	1275 m	1276 m	1277 (8)	1306	1275(21.0)	1318	1275(21.0)					ν (N3–C4) (20), ν (C10–C11) (12)
	1251 m	1254 m	1253 (8)					1299	1256(1.4)	1303	1261(13.6)	β (C5–H9) (30), ν (C4–C5) (15)
ν_{15}	1235 m	1236 s	1237 sh					1268	1234(1.4)	1265	1230(0.7)	β (C2–H7) (30), ν (N1–C5) (13)
	1222 m	1226 m 1222 m	1226 (1)	1258	1218(4.4)	1251	1218(4.4)					β (C12–H16) (21), β (C2–H7) (20)
ν_{16}	1204 m	1209 w 1205 m	1207(2)					1236	1199(2.6)	1229	1190(10.2)	ν (C8–O13) (16), β (C10–H14) (14)
	1183 sh	1190 w	1191 (3)	1224	1183(13.1)	1218	1183(13.1)					β (C5–H9) (18), β (C2–H7) (16), β (C10–H14) (13)
ν_{17}	1162 s	1169 s 1167 vs	1165 (4)	1185	1145(20.0)	1185	1145(19.9)	1188	1147(15.3)	1179	1140(12.9)	ν (C8–O13) (22), ν (C12–O13) (21), β(C12–H16) (18)
ν_{18}	1120 vs	1125 w 1120 s	1123 (6) 1115 sh	1132	1085(8.4)	1127	1084(8.5)	1151	1112(18.4)	1153	1115(20.6)	ν (C4–C5) (40), ν (C2–N1) (26)
ν_{19}	1081 vs	1082 s	1083 (4)					1117	1080(20.8)	1121	1080(15.4)	ν (C2–N1) (20), β (N1–H6) (18)
	1071 w	1071 vs	1073 (6)	1113	1072(13.4)	1115	1066(13.7)					β (N1–H6) (34), ν (C2–N3) (26)
ν_{20}	1067 s	–	–	1103	1059(14.7)	1097	1058(15.1)	1102	1061(15.4)	1097	1056(13.1)	ν (C12–O13) (54), ν (C10–C11) (13)
ν_{21}	1050 m	–	–	1082	1040(26.5)	1072	1040(26.2)	1088	1054(22.4)	1084	1048(23.8)	ν (C2–N3) (29), β (N1–H6) (18)
ν_{22}	1006 *vs*	1016 w 1006 *vs*	1010 (4)	1036	992(36.4)	1023	991(36.2)	1033	1001(41.5)	1031	1000(24.7)	β (C10–H14) (28), ν (C10–C11) (27), β (C11–H15) (24)
ν_{23}	971 s 964 m	973 m 965w	971 (10) 966 sh					994	976(4.8)	984	9669(23.3)	βr_1(i) (35), ν (C8–O13) (15)

Table 5. (*Continued*)

				4-FI				5–FI				
				anti		*syn*		anti		syn		
	IR R. T.[a]	IR L.T.[b]	Raman	Calc.[c]	SQM[d]	Calc.[c]	SQM[d]	Calc.[c]	SQM[d]	Calc[c].	SQM[d]	Assignment[e]
	942 m	945 m	943 (1)	961	942(3.3)	964	942(3.3)					$\beta R_1(i)$ (51), $\beta R_2(i)$ (14)
ν_{24}	–	939 m		947	941(0.9)	950	941(0.9)					$\beta R_2(i)$ (26), $\beta R_1(i)$ (22)
	917 sh	916 w	916 (1)					935	924(0.0)	938	927(10.2)	$\beta R_1(i)$ (51), $\beta R_2(i)$ (12)
ν_{25}			892(3)	903	897(15.9)	903	897(15.3)	903	897(10.9)	903	897(13.1)	$\beta R_1(f)$ (52), $\beta R_2(f)$ (30)
ν_{26}	885 s	884 s	885 (3)	900	890(10.7)	898	890(11.2)	899	890(14.9)	898	889(1.9)	$\beta R_2(f)$ (37), $\beta R_1(f)$ (24)
ν_{27}	456 w	457 w	455 (1)	459	453(0.5)	462	453(0.5)	453	448(5.2)	454	449(6.4)	β (C8–C4) (72)
ν_{28}	404 w	402 m	404 (2)	394	383(0.3)	393	383(0.3)	393	383(0.1)	397	386(0.1)	ν (C4–C8) (44) $\beta R_1(i)$(18)
ν_{29}			160 (4)	159	136(6.7)	140	138(6.7)	144	143(1.6)	142	142(3.7)	γ (C8–C4) (64)
							Symmetry A″					
ν_{30}	868 sh	871 w 864 sh	871(1)	879	870(0.4)	879	870(0.3)	869	860(0.1)	877	868(0.0)	γ (C11–H15) (48), γ (C10–H14) (28), $\tau R_1(f)$ (13)
ν_{31}	830 s	833 w 830 s	826 sh					846	826(19.5)	836	820(22.0)	γ (C5–H9) (77)
	813 m	816 m	–	825	815(7.1)	825	815(5.5)					γ (C10–H14) (51), γ (C11–H15) (16)
ν_{32}	800 m	798 m	800 sh	813	806(45.2)	815	805(47.0)	800	799(33.9)	807	797(44.9)	γ (C2–H7) (73), $\tau R_1(i)$ (12)
ν_{33}	776 vs 769 m	777 s 771 s	775 (2)					785	776(11.4)	797	788(3.1)	γ (C10–H14) (70), γ (C2–H7) (10)
	750 vs	753 vs	750 (4)	768	752(26.5)	767	752(26.6)					γ (C5-H9) (34), $\tau R_2(i)$ (25)
ν_{34}	725 vs	725 vs	731 sh	747	720(41.1)	729	720(40.1)	734	724(68.9)	727	717(58.8)	γ (C12–H16) (68), γ (C11–H15) (14)
ν_{35}	702 w	702 m	693 (3)	708	691(15.9)	706	691(16.2)					τwis_{Ring} (33), $\tau R_2(i)$ (28)
	685 m 668 m	686 s	685 (1)					688	668(7.9)	678	659(14.1)	τwis_{Ring} (37), $\tau R_2(f)$ (27) γ (C8–C4) (48), τwis_{Ring} (20)
ν_{36}	656 s	657 s	655 (1)					667	647(8.5)	670	650(3.9)	$\tau R_1(i)$ (77), τR_2 (i) (17)
	652 m	652 s	657 (1)	673	648(3.1)	666	647(3.1)					τR_2 (f) (23), τR_1 (i) (22)
ν_{37}	635 s	635 s	636 (1)					640	621(2.4)	643	625(3.9)	τR_2 (i) (29), τR_2 (f) (21)
	621 m	624 m 622 m	622 (1)	643	620(3.5)	638	620(3.4)					τR_1 (i) (34), τR_2 (i) (29)
ν_{38}	591 vs	594 vs 591 vs	596 (1) 593 (1)	607	586(6.3)	605	586(6.4)	599	580(10.1)	599	581(8.3)	τR_1 (f) (66), τR_2 (f) (23)
ν_{39}	534 w	534 w	–							542	534(82.8)	γ (N1–H6) (38), τR_2 (i) (27)
	498 w	497 s	–	523	497(104.5)	505	497(104.5)					γ (N1–H6) (64), τR_1 (i) (30)
	464 w	466 w	465 (2)					479	471(79.9)			γ (N1–H6) (64), τR_2 (i) (24)
ν_{40}	337 w		336 (2)	331	320(0.5)	330	320(0.5)	318	300(1.1)	314	305(1.1)	τwis_{Ring} (42), $\tau R_2(i)$ (32)
ν_{41}			123 (8)	131	119(8.0)	121	117(8.2)	118	109(0.2)	120	116(0.2)	β (C4–C8) (65)
ν_{42}			97 (10)	52	66(5.9)	68	66(0.0)	32	31(2.3)	45	42(5.2)	Butt. (87)

s, strong; m, medium; w, weak; *v*, very; sh, shoulder; br, broad; f, furyl; i, imidazoles; ν, stretching; β, in the plane deformation; βR, ring deformation; γ, out of plane deformation; τR, ring torsion; Butt, butterfly

[a] RT–Room temperature.

[b] LT–Low temperature.

[c] Theoretical value (B3LYP/6-311++G**).

[d] From scaled quantum mechanical force field; the infrared intensities are given in parenthesis and expressed in km mol^{-1}.

[e] PED is given in parenthesis and contributions only ≥10% were considered.

and they could be associated with the calculated value for the normal ν_8 mode at 1521 and 1514 cm^{-1} for the *syn* and *anti* conformers of the **5-FI** tautomer, respectively. The experimental vibrational spectrum fits fairly well with that predicted by the theoretical model as shown in Figs 2 and 3, and the calculated initial RMSD values obtained from a comparison between the theoretical (B3LYP/6-311++G**) and experimental wavenumbers for the *anti* and *syn* conformers are 53 and 47.7 cm^{-1} for the **4-FI** tautomer and 68 cm^{-1} for both conformers of the **5-FI** tautomer. After the scaling process of the force constants, the RMSD values decrease to 13 cm^{-1} for all conformers of the studied isomeric species. This reasonable standard deviation value, taking into account the complexity of the analyzed sample and that the scale factors were taken directly from those of Rauhut and Pulay,[14,15] allowed us to compare with an acceptable level of agreement between the theoretical spectra and the experimental ones in order to carry out a complete assignment of the vibrational normal modes of 4(5)-(2′-furyl)-imidazole. The comparison of the theoretical infrared and Raman spectra for the two conformations of both isomeric species with the corresponding experimental spectrum at ambient temperature is shown in Figs 2 and 3.

Assignment of the bands

Region 4000–3000 cm^{-1}

The broad band observed in the infrared spectrum at 3442 cm^{-1} is assigned to the N–H stretching mode for both tautomers of 4(5)-(2′-furyl)-imidazole because they are expected at 3444 and 3443 cm^{-1}. The group of bands in the 3150–3000 cm^{-1} region was attributed to the C–H stretching modes as shown in Table 5.

Region 2000–1000 cm^{-1}

This region is the most complex because the skeletal ring modes are strongly coupled and for this reason it is difficult to assign the bands of **5-FI** tautomer. The band of relatively high intensity in the infrared and Raman spectra at 1638 cm^{-1}, which appears perfectly split at LT, is assigned, by comparison with the theoretical results, to the stretching C=C modes. The other two stretching C=C modes were assigned to the IR bands at 1538/1534 cm^{-1} (in the Raman spectra both at 1540 cm^{-1}) and 1438/1430 cm^{-1} for the **5-FI** tautomer and at 1516 and 1467 cm^{-1} (in the Raman spectra at 1520 and 1468 cm^{-1}) for the **4-FI** tautomer. The second band in the pair is split at LT at 1445/1441 cm^{-1} and 1434/1431 cm^{-1}, respectively. As predicted by the calculations, the band in the infrared spectrum of the solid substance at 1491 cm^{-1} (in the Raman spectrum at 1492 cm^{-1}) is assigned to the C=N stretching modes. The theoretical calculations predict that the stretching modes of the imidazole ring appear at different wavenumbers for each one of the isomers, and accordingly the three stretching C–N modes for the **4-FI** tautomer are assigned to the IR bands at RT at 1400, 1275 and 1050 cm^{-1} and the Raman peaks at 1401 and 1277 cm^{-1}, respectively. These modes corresponding to the **5-FI** tautomer are difficult to assign, given the complexity of the potential energy distribution (PED) contributions for each one of the conformers; only one of them is clearly predicted by the calculations and it is assigned to the IR band at 1081 cm^{-1}. The shoulder located in the infrared spectrum at RT at 1378 cm^{-1}, observed at low temperature as a weak band at the same wavenumber and in the Raman spectrum at 1371 cm^{-1}, and in comparison with the furane molecule[53] and with the results of the theoretical calculations, is assigned to the C–C stretching mode of the furan ring for the two tautomers. The pair of bands located at 1162 and 1067 cm^{-1}, which is observed in the Raman spectrum as only one band at 1165 cm^{-1}, is assigned, based on prediction by the calculations for their intensity as well as on comparison with the studied molecules,[50,51] to the stretching C–O modes for both **4-FI** tautomers.

The in-plane C–H deformation modes are expected between 1300 and 1000 cm^{-1}, as predicted by the calculations and in comparison with those observed for similar molecules.[50,51] In this case, the bands located in the infrared spectrum at 1307/1304, 1222, 1183, 1162, and 1006 cm^{-1} and of which four only are observed in the Raman spectrum at 1308/1303, 1226, 1191, and 1010 cm^{-1} are assigned to the five modes of the **4-FI** tautomer, while the bands at 1251, 1235, 1204 and 1006 cm^{-1} are assigned to the **5-FI** tautomer. The in-plane N–H deformation band is predicted by the calculations for both tautomers, with an average difference of 10 cm^{-1}, for the IR band at 1071 cm^{-1} (in the Raman spectrum at 1073 cm^{-1}) and at 1081 cm^{-1} (in the Raman spectrum at 1083 cm^{-1}), and they are assigned respectively to this mode for the **4-FI** and **5-FI** tautomers.

Region below 1000 cm^{-1}

The pair of bands located in the infrared spectrum at RT at 971 and 964 cm^{-1} (in the Raman spectrum at 971 and 966 cm^{-1}) are assigned to the expected imidazol ring deformation (βR(i)) for the **5-FI** tautomer, while the bands at 942 and 939 cm^{-1} (in the Raman spectrum observed as a single band at 943 cm^{-1}) are assigned to these modes for the **4-FI** tautomer. According to the prediction of the theoretical calculations and from comparison with the wavenumbers reported for the furan molecule,[53] the two furan ring deformation modes (β(R(f)) are assigned for both tautomers to the IR and Raman bands at 892 and 885 cm^{-1}.

The five C–H out-of-plane deformations predicted by calculations and observed in the molecules previously studied[50,51] lie in the region between 870 and 700 cm^{-1}. From these observations, the shoulder at 868 cm^{-1} and the observed bands in the infrared spectrum at RT at 813, 800, 750, and 725 cm^{-1}, of which only four are observed in the Raman spectrum at 871, 800, 750, and 731 cm^{-1}, are assigned to those modes of the **4-FI** tautomer. For the **5-FI** molecule, three of those bands are assigned to the same wavenumbers as the previous species (868, 800, and 725 cm^{-1}), and the two remaining modes are assigned to the IR bands at 830 and 776 cm^{-1} and the Raman bands at 826 and 775 cm^{-1}.

For both tautomers, the two torsional modes of the imidazol ring are predicted by the calculations to lie between 700 and 660 cm^{-1} with significant differences among them. The bands in the infrared spectrum at 702 and 652 cm^{-1} and in the Raman spectrum at 693 and 657 cm^{-1} are associated with these modes for the **4-FI** tautomer, while the corresponding bands are at 656 and 635 cm^{-1} (655 and 636 cm^{-1}) in the **5-FI** tautomer. As predicted by the calculations, the two the furan ring torsional modes are assigned to the IR bands at 621 and 591 cm^{-1} (in the Raman spectrum at 622 and 596 cm^{-1}) for the **4-FI** tautomer and at 685 and 591 cm^{-1} in the infrared and Raman spectra of the **5-FI** tautomer.

The theoretical calculations predict the N–H out-of-plane deformation for each conformer of the tautomer species at different wavenumbers and slightly displaced with respect to each other. Therefore, the IR bands at 534 and 464 cm^{-1} are assigned to these modes for both conformers of the **5-FI** tautomer, while the band in the infrared spectrum at 498 cm^{-1} for other tautomer is assigned to these modes.

Table 6. Comparison of the force constants of the **4-FI** and **5-FI** with the corresponding to 2-(2′-furyl)-1*H*-imidazole

	2-(2′-Furyl)-1*H*-Imidazole		4-(2′-furyl)-Imidazole		5-(2′-furyl)-Imidazole	
Description	*anti*	*syn*	*anti*	*syn*	*anti*	*syn*
f (C–C)$_{int}$	5.87	5.44	5.28	5.28	5.35	5.38
f (C–C)	6.14	5.44	5.37	6.08	5.38	5.38
f (C═C)$_{imidazole}$	7.98	7.49	6.90	5.18	6.77	6.73
f (C═C)$_{furan}$	8.22	7.99	7.41	7.30	7.35	7.39
f (C–N)	6.73	6.35	5.92	6.40	5.95	6.00
f (C═N)	7.25	7.92	7.93	8.78	7.78	7.71
f (N–H)	6.55	6.55	6.56	6.35	6.56	6.54
f (C–H)	5.23	5.23	5.34	5.21	5.32	5.32
f (C–O)	6.38	6.36	5.29	5.85	5.35	5.23
β_R	0.37	0.47	0.41	0.47	0.40	0.41
τ_R	0.66	0.68	0.62	0.61	0.62	0.63
f (β C–H)	0.49	0.48	0.44	0.59	0.45	0.45
f (β N–H)	0.55	0.47	0.42	0.43	0.43	0.42
f (γ C–H)	0.36	0.37	0.37	0.37	0.36	0.39
f (γ N–H)	0.13	0.19	0.20	0.21	0.14	0.18
f ($\tau w R$ing)	0.03	0.10	0.10	0.07	0.03	0.04

Below 460 cm^{-1} the theoretical calculations predict for both tautomers six vibrational normal modes associated to the inter-rings modes, such as γ(C–C)$_{inter-rings}$, β(C–C)$_{inter-rings}$, the butterfly mode and τ (C–C)$_{inter-rings}$ (see Figure 5). However, only two of them are observed in the infrared spectrum and the remaining ones are in the Raman spectrum. The two bands observed in the IR spectrum at 456 cm^{-1} and in the Raman spectrum at 160 cm^{-1} are assigned to β(C–C)$_{inter-rings}$, for both tautomers. The (C–C)$_{inter-rings}$ stretching is assigned to the Raman band at 404 cm^{-1}. The three bands observed in the Raman spectrum at 336, 123 and 97 cm^{-1}, according to their wavenumbers and their corresponding intensities of the calculations, as well as from comparison with the previously studied molecules,[50,51,54] are attributed as follows: the first one to the C–C out-of-plane deformation, the second to the butterfly mode and the remaining one to the torsion inter-rings.

Force field

The corresponding force constants for the experimentally studied 4(5)-(2′-furyl)-imidazole were estimated using the scaling procedure of Pulay *et al.*,[31,32] as mentioned before. The force constants appearing in Table 6 expressed in terms of simple valence internal coordinates were calculated from the corresponding scaled force fields. It is interesting to compare the principal force constants calculated at the B3LYP/6-311++G** levels for both tautomers with those corresponding to the 2-(2′-furyl)-1*H*-imidazole.[34] In general, the calculated force constant values for the *anti* and *syn* conformers for both tautomers are approximately the same. The most important difference is found for the C═C, C–N, and C–O stretching force constants, which are higher for the 2-(2′-furyl)-1*H*-imidazole compound. This observation can be explained by means of the calculated bond lengths (Table 2) because they are larger for these tautomers than those observed for the 2-(2′-furyl)-1*H*-imidazole molecule. The values of the remaining force constants do not present significant differences.

Conclusions

- The 4(5)-(2′-furyl)-imidazole molecule was synthesized and characterized by GC-MS as well as by infrared and Raman spectroscopic techniques in the solid state and also by NMR in solution. The following points may be noted:
- The present work shows the existence of equilibrium between the **4-FI** and **5-FI** tautomers of this molecule, which were evaluated at lower temperature.
- The presence of **4-FI** and **5-FI** tautomers was detected in the IR spectrum, and a complete assignment of the vibrational modes was accomplished.
- The calculations suggest the existence of two molecular *anti* and *syn* conformations for each of them, both of the C_s symmetry.
- An SQM force field was obtained for *anti* and *syn* conformers of **4-FI** and **5-FI** tautomeric structures after adjusting the theoretically obtained force constants to minimize the difference between the observed and calculated wavenumbers.

Acknowledgements

We thank Prof. Tom Sundius for authorizing the use of the MOLVIB Program. We also thank CONICET (Consejo Nacional de Investigaciones Científicas y Técnicas) and CIUNT (Consejo de Investigaciones de la Universidad Nacional de Tucumán) for financial support.

Supporting information

Supporting information may be found in the online version of this article.

References

[1] K. Schofield, M. R. Grimment, B. R. T. Keene, *Heteroaromatic Nitrogen Compounds, The Azoles*, Cambridge University Press: London, New York, **1976**.
[2] J. Elguero, C. Marzin, R. Katritzky, P. Linda, *Adv. Heterocycl. Chem. Suppl.* **1976**, *1*, 280.
[3] B. I. Khristich, *Khim. Geterotsikl. Soedin.* **1970**, 1683.
[4] M. R. Grimment, *Sciences of Synthesis: Honben-Weyl Methods on Molecular Transformation*, vol 12, (Ed.: R. Neier), Georg Thieme Verlog: New York, **2002**, pp 325, Chapt. 3.

[5] M. Charton, *J. Org. Chem.* **1979**, *44*, 903.
[6] M. Charton, *J. Chem. Soc. B* **1969**, 1240.
[7] PatentStorm LLC, United States Patent no., 5559141.
[8] F. Bellina, S. Cauteruccio, R. Rossi, *J. Org. Chem.* **2007**, *72*(22), 8543.
[9] S. A. Popov, R. V. Andreev, G. V. Romanenko, V. I. Ovcharenko, V. A. Reznikov, *J. Mol. Struct.* **2004**, *697*(1–3), 49.
[10] K. Sztanke, S. Fidecka, E. K dzierska, Z. Karczmarzyk, K. Pihlaja, D. Matosiuk, *Eur. J. Med. Chem.* **2005**, *40*(2), 127.
[11] F. O. Talbot, L. C. Snoek, N. A. Macleod, P. Butz, J. P. Simons, R. T. Kroemer, Lasers for Science Facility Programme – Chemistry, **2002**.
[12] J. P. Simons, E. G. Robertson, M. R. Hockridge, Science – Lasers for Science Facility – Chemistry, **1999**.
[13] J. Vázquez, J. J. López González, L. Ballester, J. Boggs, *J. Mol. Struct.* **1997**, *393*, 97.
[14] G. Rauhut, P. Pulay, *J. Phys. Chem.* **1995**, *99*, 3093.
[15] G. Rauhut, P. Pulay, *J. Phys. Chem.* **1995**, *99*, 1457.
[16] F. Kalincsák, G. Pongor, *Spectrochim. Acta A* **2002**, *58*, 999.
[17] A. E. Reed, L. A. Curtis, F. Weinhold, *Chem. Rev.* **1988**, *88*(6), 899.
[18] J. P. Foster, F. Weinhold, *J. Am. Chem. Soc.* **1980**, *102*, 7211.
[19] A. E. Reed, F. Weinhold, *J. Chem. Phys.* **1985**, *83*, 1736.
[20] E. D. Gledening, J. K. Badenhoop, A. D. Reed, J. E. Carpenter, F. F. Weinhold, *NBO 3.1*, Theoretical Chemistry Institute, University of Wisconsin: Madison, WI, **1996**.
[21] R. F. W. Bader, *Atoms in Molecules, A Quantum Theory*, Oxford University Press: Oxford, **1990**, ISBN: 0198558651.
[22] F. Biegler-Köning, J. Schönbohm, D. Bayles, AIM2000; A program to analyze and visualize atoms in molecules. *J. Comput. Chem.* **2001**, *22*, 545.
[23] A. E. Vogel, *Practical Organic Chemistry*, (3rd edn), Longman. London, **1997**, p 823.
[24] B. E. Love, P. S. Raje, T. C. Williams, II *Synlett* **1994**, 493.
[25] R. Ten Have, M. Huisman, A. Meetsma, A. M. Van Leusen, *Tetrahedron* **1997**, *53*(33), 11355.
[26] M. J. Frisch, G. W. Trucks, H. B. Schlegel, G. E. Scuseria, M. A. Robb, J. R. Cheeseman, J. A. Montgomery Jr., T. Vreven, K. N. Kudin, J. C. Burant, J. M. Millam, S. S. Iyengar, J. Tomasi, V. Barone, B. Mennucci, M. Cossi, G. Scalmani, N. Rega, G. A. Petersson, H. Nakatsuji, M. Hada, M. Ehara, K. Toyota, R. Fukuda, J. Hasegawa, M. Ishida, T. Nakajima, Y. Honda, O. Kitao, H. Nakai, M. Klene, X. Li, J. E. Knox, H. P. Hratchian, J. B. Cross, C. Adamo, J. Jaramillo, R. Gomperts, R. E. Stratmann, O. Yazyev A. J. Austin, R. Cammi, C. Pomelli, J. W. Ochterski, P. Y. Ayala, K. Morokuma, G. A. Voth, P. Salvador, J. J. Dannenberg, V. G. Zakrzewski, S. Dapprich, A. D. Daniels, M. C. Strain, O. Farkas, D. K. Malick, A. D. Rabuck, K. Raghavachari, J. B. Foresman, J. V. Ortiz, Q. Cui, A. G. Baboul, S. Clifford, J. Cioslowski, B. B. Stefanov, G. Liu, A. Liashenko, P. Piskorz, I. Komaromi, R. L. Martin, D. J. Fox, T. Keith, M. A. Al-Laham, C. Y. Peng, A. Nanayakkara, M. Challacombe, P. M. W. Gill, B. Johnson, W. Chen, M. W. Wong, C. Gonzalez, and J. A. Pople, *Gaussian 03, Revision B.01*, Gaussian, Inc.: Pittsburgh, PA, **2003**.
[27] D. Becke, *J. Chem. Phys. Rev.* **1993**, *98*, 5648.
[28] C. Lee, W. Yang, R. G. Parr, *Phys. Rev.* **1988**, *B37*, 785.
[29] T. Sundius, *J. Mol. Struct.* **1990**, *218*, 321.
[30] T. Sundius, *Vib. Spectrosc.* **2002**, *29*, 89.
[31] P. Pulay, G. Fogarasi, F. Pang, E. Boggs, *J. Am. Chem. Soc.* **1979**, *101*(10), 2550.
[32] P. Pulay, G. Fogarasi, G. Pongor, J. E. Boggs, A. Vargha, *J. Am. Chem. Soc.* **1983**, *105*, 7037.
[33] R. Ditchfield, *Mol. Phys.* **1974**, *8*, 397.
[34] A. E. Ledesma, S. A. Brandán, J. Zinczuk, O. E. Piro, J. López González, A. Ben Altabef., *J. Phys. Org. Chem.* **2008**, *21*(12), 1086.
[35] M. Winter, Web elements, http://www.webelements.com.
[36] H. Xile, K. Meyer, *J. Am. Chem. Soc.* **2004**, *126*, 16322.
[37] N. O. Pekmez, M. Can, A. Yildiz, *Acta Chim. Slov.* **2007**, *54*, 131.
[38] W. Brugel, *Handbook of NMR Spectral Parameters*, vols. 1–3, Heyden: Philadelphia, **1979**.
[39] A. E. Ledesma, J. Zinczuk, J. López González, A. Ben Altabef, S. A. Brandán, *J. Mol. Struct.* **2009**, DOI 10.1016/j.molstruct.2009.01.058.
[40] R. F. W. Bader, *J. Phys. Chem. A* **1998**, *102*, 7314.
[41] P. L. A. Popelier, *J. Phys. Chem. A* **1998**, *102*, 1873.
[42] U. Koch, P. L. A. Popelier, *J. Phys. Chem.* **1995**, *99*, 9747.
[43] G. L. Sosa, N. Peruchena, R. H. Contreras, E. A. Castro, *J. Mol. Struct. (THEOCHEM)* **1997**, *401*, 77.
[44] G. L. Sosa, N. Peruchena, R. H. Contreras, E. A. Castro, *J. Mol. Struct. (THEOCHEM)* **2002**, *577*, 219.
[45] S. Wojtulewski, S. J. Grabowski, *J. Mol. Struct.* **2003**, *645*, 287.
[46] S. Wojtulewski, S. J. Grabowski, *J. Mol. Struct.* **2003**, *621*, 285.
[47] S. J. Grabowski, *Monatsh. Chem.* **2002**, *133*, 1373.
[48] C. Vizioli, M. C. Ruiz de Azúa, C. G. Giribet, R. H. Contreras, L. Turi, J. J. Dannenberg, I. D. Rae, J. A. Weigold, M. Malagoli, R. Zanasi, P. Lazzeretti, *J. Phys. Chem.* **1994**, *98*, 8858.
[49] J. J. Dannenberg, Y. D. Rae, J. A. Weingold, M. Malagoli, R. Zanasi, P. Lazzeretti, *J. Phys. Chem.* **1994**, *98*, 8858.
[50] J. Zinczuk, A. E. Ledesma, S. A. Brandán, O. E. Piro, J. J. López-González, A. Ben Altabef, *J. of Phys. Org. Chem* **2009**, *21*, 1.
[51] A. E. Ledesma, J. Zinczuk, A. Ben Altabef, J. López González, S. A. Brandán, *J. Raman Spectrosc.* **2009**, DOI 10.1002/jrs.2219.
[52] A. Toyama, K. Ono, S. Hashimoto, H. Takeuchi, *J. Phys. Chem. A* **2002**, *106*, 3403.
[53] T. D. Klots, R. D. Chirrido, W. V. Stele, *Spectrochim. Acta A* **1994**, *50*, 765.
[54] S. T. King, *J. Phys. Chem.* **1970**, *74*, 2133.

